Quantitative measurements of absorption spectra in scattering media by low-coherence spectroscopy

Nienke Bosschaart,[1,*] Maurice C. G. Aalders,[1] Dirk J. Faber,[1,2] Jelmer J. A. Weda,[1] Martin J. C. van Gemert,[1] and Ton G. van Leeuwen[1,3]

[1]*Biomedical Engineering and Physics, Academic Medical Center, University of Amsterdam, P.O. Box 22700, NL-1100 DE Amsterdam, The Netherlands*

[2]*Ophthalmology Department, Academic Medical Center, University of Amsterdam, P.O. Box 22700, NL-1100 DE Amsterdam, The Netherlands*

[3]*Biophysical Engineering Group, MIRA Institute for Biomedical Technology and Technical Medicine, University of Twente, P.O. Box 217, NL-7500 AE Enschede, The Netherlands*

**Corresponding author: n.bosschaart@amc.uva.nl*

Received July 27, 2009; revised October 19, 2009; accepted November 18, 2009; posted November 10, 2009 (Doc. ID 114864); published November 30, 2009

Low-coherence spectroscopy (LCS) is a spectroscopic method that allows for quantitative and localized assessment of absorption spectra by combining reflection spectroscopy with low-coherence interferometry. We describe absorption coefficient (μ_a) measurements by LCS in tissue simulating phantoms with varying scattering and absorbing properties. We used LCS in the 455–680 nm wavelength range with a spectral resolution of 8 nm to obtain μ_a spectra with ±0.5 mm^{-1} accuracy. We conclude that LCS is a promising technique for the *in vivo* determination of tissue chromophore concentrations. © 2009 Optical Society of America

OCIS codes: 170.6510, 300.1030, 030.1640.

Optical spectroscopy for *in vivo* determination of chromophore concentrations (e.g., hemoglobin and bilirubin) offers an alternative to frequent and invasive drawing of blood followed by time-consuming laboratory analysis. However, owing to lack of knowledge of the optical path in tissue, the current clinically applied spectroscopic techniques such as elastic scattering, absorption, and differential path length spectroscopy [1–3] depend on photon path-length models for the determination of absolute chromophore concentrations. Another limitation is the lack of localization [1,2], i.e., the measured signal originates from a large volume, which makes it difficult to confine the measurement to a preferred target volume such as the microcirculation in the skin. *Quantitative* (i.e., absolute concentrations) and localized spectroscopic measurements of tissue chromophores require knowledge of (or control over) the path length of light in tissue, because then tissue absorption coefficients, which are directly related to chromophore concentrations, can be calculated using Beer's law.

In this Letter, we demonstrate for the first time (to our knowledge) that low-coherence spectroscopy (LCS) allows for quantitative assessment of absorption spectra in scattering media as a first step toward noninvasive *in vivo* tissue chromophore concentration measurements. LCS combines reflection spectroscopy with low coherence interferometry (LCI) to control the path length of the detected light. To validate this method, we performed *in vitro* measurements of absorption coefficient spectra on samples with known absorption and scattering properties.

LCS is an extension of LCI and can therefore be placed alongside techniques such as optical coherence tomography (OCT) and path-length-resolved optical Doppler measurements [4]. LCS recovers spectroscopic information at controlled path lengths from the sample, similar to spectroscopic OCT (sOCT) [5–8]. However, LCS is fully optimized for spectroscopy, instead of tomography. This allows a system design with high spectral resolution at the sacrifice of spatial resolution. Also, sampling intervals can be optimized for spectroscopic purposes, and the measurement volume can be enlarged for better signal-to-noise ratios. Our LCS system operates in the visible wavelength range, because of the distinct features of important chromophores such as bilirubin and hemoglobin in this region, compared with the near-IR region (NIR). Hence, chromophore concentration alterations induce more pronounced changes in absorption. In sOCT, spectroscopy is combined with imaging, which limits the available wavelengths to the NIR to obtain sufficient imaging depth. Other path-length-resolved spectroscopic methods, such as time of flight [9] and phase-resolved spectroscopy [10], measure the optical path length, rather than controlling it. In addition, their range of validity is limited to large path lengths, which compromises localization.

In our current LCS implementation, backscattered power spectra $S(\ell,\lambda)$ are determined at controlled geometrical path lengths ℓ of the light in the sample as a function of wavelength λ. Our LCS system (Fig. 1) consists of a Michelson interferometer with a supercontinuum light source (SC430-4, Fianium Ltd., U.K.). The system is optimized for a bandwidth of 455–680 nm, resulting in a coherence length of ~1.5 μm. The light is focused by 25 mm focal length achromatic lenses on the sample and a piezo-driven reference mirror. Optical power at the sample is 2.5 mW. Both the sample and the reference mirror are mounted on motorized translation stages, which are used for controlling ℓ of the light in the sample ($\ell=0-2$ mm, in steps of 27 μm). Around ℓ, the signal is modulated by scanning the piezo-driven reference mirror at 23 Hz over a range of $\Delta R=30$ μm, which results in a scanning window of $\Delta\ell=2\Delta R/n\approx 44$ μm

0146-9592/09/233746-3/$15.00

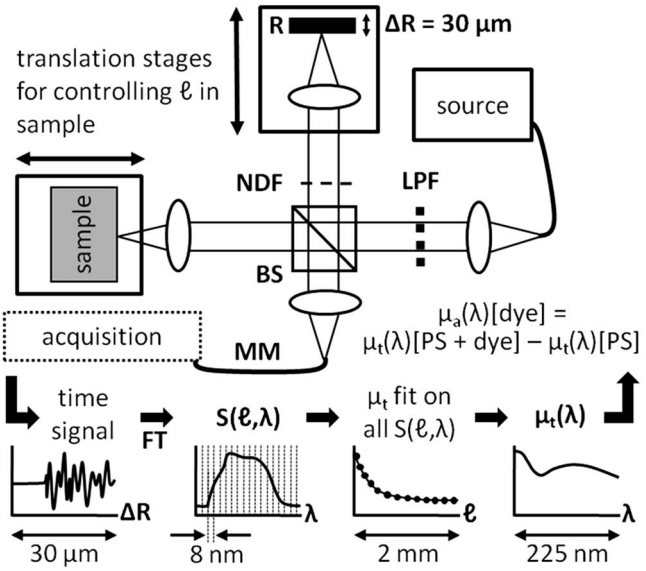

Fig. 1. LCS system (upper part) and a schematic overview of the signal processing (lower part). LPF, low-pass filter; BS, beam splitter; NDF, neutral density filter; R, piezo-driven reference mirror; ΔR, scanning range of R; MM, multimode graded index detection fiber; FT, Fourier transform; PS, polystyrene spheres; ℓ, geometrical optical path length in the sample; λ, wavelength; S, power spectrum; μ_t/μ_a, attenuation/absorption coefficient.

within the sample (with refractive index $n=1.35$ for aqueous solutions of polystyrene spheres, see below). During the measurements, ℓ is matched with the location of the focus in the sample, while taking into account the refractive-index-induced focal shift in the sample. The depth of focus of the sample arm lens is 60 μm in air.

A graded-index multimode fiber (Ø62.5 mm, M31L01 Thorlabs, USA) guides the reflected light from both arms to a photodiode (2001, New Focus, USA). Multimode detection sacrifices spatial resolution compared with single-mode detection but makes the system less sensitive to changes in sample geometry that affect the spectral bandwidth of the light coupled into the detection fiber. A schematic overview of the signal processing after acquisition is given in Fig. 1. The time signal on the detector is bandpass filtered and demodulated by a lock-in amplifier at the fixed spectral center frequency of 6690 Hz, corresponding to a wavelength of 550 nm. Per scanning window, 512 samples of amplitude and phase are digitized and multiplied by a Hanning window before applying a Fourier transform to obtain $S(\ell,\lambda)$. The frequency axis f of the Fourier spectrum is converted to wavelength using $\lambda=2v_p/f$, where v_p is the velocity of the piezo-driven reference mirror (1.84 mm/s). Correct wavelength mapping of the spectra was verified using two narrow bandpass filters at wavelengths of 510 and 577 nm. For the scanning window $\Delta\ell$ of 44 μm, the spectral resolution is given by $\Delta\lambda=\lambda^2/(n\Delta\ell)\sim 8$ nm at 680 nm.

For each geometrical path length ℓ, the average of 400 measured spectra $S(\ell,\lambda)$ is binned into wavelength regions of 8 nm to obtain equidistant data points for $S(\ell,\lambda)$. Attenuation coefficients per wavelength region $\mu_t(\lambda)$ are determined by fitting Beer's law to $S(\ell,\lambda)$ versus ℓ, using a nonlinear least-squares fitting algorithm. The accuracy in $\mu_t(\lambda)$ is quantified by the 95% confidence intervals (c.i.) of the fitted $\mu_t(\lambda)$ [5]. Spectra acquired from $\ell<80$ μm suffer from artifacts by specular reflections at the sample surface and are therefore excluded from the fits. The dynamic range, defined as the maximum of $S(\ell,\lambda)$ from a scattering sample (see below) divided by the variance of the noise in $S(\ell,\lambda)$, was 100 dB at the center wavelength and 70 dB at the spectral boundaries of 455 and 680 nm.

We prepared two sets of samples with three different concentrations of scattering polystyrene spheres (20%, 10%, and 5% dilutions from a stock of 25 mg/ml, 392 nm diameter, KI-PPS-0.4, G. Kisker GbR, Germany). Mie calculations gave an anisotropy of $g=0.78$ and scattering coefficients of 10.9 mm^{-1}, 5.5 mm^{-1} and 2.7 mm^{-1} at the center wavelength. The first set contained only the three concentrations of polystyrene spheres; the second set contained the same concentrations of polystyrene spheres as the previous set but also a fixed concentration of absorbing green dye (37.5% Ecoline #600, Royal Talens, The Netherlands). Attenuation spectra of the six solutions are shown in Fig. 2. The determined attenuation coefficients demonstrate the feasibility of LCS to extract the $\mu_t(\lambda)$ with an accuracy of ± 0.25 mm^{-1}. For the nonabsorbing samples (only polystyrene spheres), the $\mu_t(\lambda)$ scale linearly with the concentration and all lie within the range of scattering coefficients of tissues [11].

The attenuation coefficient is the sum of the scattering and absorption coefficients $\mu_s(\lambda)$ and $\mu_a(\lambda)$ of the sample. A straightforward method to derive $\mu_a(\lambda)$ from the measured $\mu_t(\lambda)$ from the samples with dye, is by subtracting $\mu_s(\lambda)$ from $\mu_t(\lambda)$, where $\mu_s(\lambda)$ is obtained from the nonabsorbing sample with identical $\mu_s(\lambda)$ (the same concentration of polystyrene spheres without dye). The resulting absorption spectra of the green dye derived from the three pairs of scattering samples are shown in Fig. 3. Owing to error propagation of the 95% c.i. in the subtraction, the accuracy for $\mu_a(\lambda)$ is approximately twice the accuracy of the $\mu_t(\lambda)$ determination (± 0.5 mm^{-1}). The three spectra

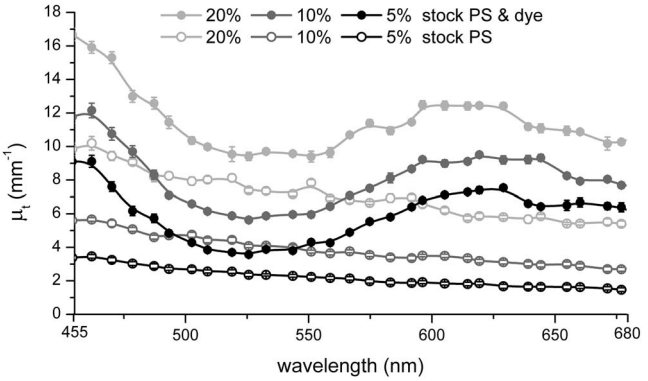

Fig. 2. Attenuation spectra for three concentrations of polystyrene spheres (PS) with and without dye. Error bars represent the 95% c.i. of the fitted values. The lines through the data points are drawn as a guide to the eye.

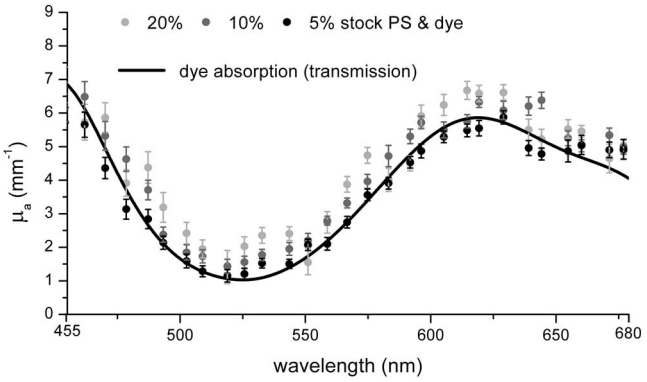

Fig. 3. Absorption spectra for three samples with varying concentrations of PS but constant concentration of absorbing dye. Error bars represent the 95% c.i. of the fitted values.

overlap within 2 mm^{-1}, which suggests that our method of determining $\mu_a(\lambda)$ holds for a broad range of scattering coefficients. Furthermore, the spectra show good agreement within 1.5 mm^{-1} with $\mu_a(\lambda)$ of the dye only (Fig. 3, solid curve) as determined in a separate transmission measurement by a spectrograph (USB4000, Ocean Optics, USA). Brownian motion of the polystyrene spheres causes Doppler broadening of the LCS spectra. Adequate comparison with $\mu_a(\lambda)$ in transmission requires convolution of the latter with a Lorentzian with a line width of 167 Hz, corresponding to the Doppler frequency distribution of the Brownian motion in the samples [4,12].

In the preceding analysis of $\mu_a(\lambda)$ we assumed that the LCS signal from the nonabsorbing samples decays exponentially with $\mu_s(\lambda)\ell$. Because our detection geometry is not optimized to reject multiple scattered light (weak confocality because of low-NA optics and the multimode detection fiber), the observed decay with ℓ can be shallower than that predicted by $\mu_s(\lambda)$. The subtraction of $\mu_t(\lambda)$ from a nonabsorbing sample can still be applied, because absorption takes place along the photon's controlled path and therefore attenuates according to Beer's law [4,13]. The wavelength dependence of the refractive index causes dispersion of the time signal. This leads to an increase of the coherence length from 1.5 μm to 20.7 μm when the path length is set at 2 mm. Since the total dispersed signal (20.7 μm) will still be sampled within our scanning window of 44 μm, sample dispersion will not affect the power spectrum and hence our calculation of $\mu_t(\lambda)$.

The current accuracy of ± 0.5 mm^{-1} will be sufficient to measure biological variation in absorption, e.g., a 6% oxygenation change in full blood in our wavelength range [11]. However, the variation in the absorption spectra in Fig. 3 suggest that the accuracy may be worse than predicted by the 95% c.i. Thus to improve the clinical value, the accuracy must be improved. Furthermore, obtaining a reference spectrum may be challenging *in vivo*, but alternative methods to separate scattering and absorption from a single attenuation profile have been proposed [2,6].

Whereas in this Letter $\mu_a(\lambda)$ is measured in nonlayered, homogeneous samples, LCS has the potential to measure $\mu_a(\lambda)$ in individual layers of layered media such as human skin. The controlled path length and the confined measurement volume owing to the confocality of the system, in principle allow to measure within a layer of choice. In complex media, where more than one chromophore contributes to the measured $\mu_a(\lambda)$, methods such as multivariate analysis [1] are required to obtain the contribution of each individual chromophore.

In conclusion, we present absorption spectra from backscattered signals of polystyrene sphere solutions with green absorbing dye, with $\mu_s(\lambda)$ and $\mu_a(\lambda)$ within the physiological range of tissue. Our method applies for a broad range of scattering coefficients and agrees with transmission spectroscopy. Compared with other spectroscopic techniques, LCS controls the path length of the detected light inside a sample, which enables both quantitative and potentially localized measurements of absorption coefficients. Since absorption coefficients are directly related to chromophore concentrations, LCS is a promising technique for *in vivo* determination of tissue chromophore concentrations in individual tissue layers.

This research is funded by personal grants in the Vernieuwingsimpuls program (MCGA: AGT07547, DJF: AGT07544) by the Netherlands Organization of Scientific Research (NWO) and the Technology Foundation STW.

References

1. P. Rolfe, Annu. Rev. Biomed. Eng. **2**, 715 (2000).
2. M. G. Nichols, E. L. Hull, and T. H. Foster, Appl. Opt. **36**, 93 (1997).
3. A. Amelink, H. J. C. M. Sterenborg, M. P. L. Bard, and S. A. Burgers, Opt. Lett. **29**, 1087 (2004).
4. B. Varghese, V. Rajan, T. G. van Leeuwen, and W. Steenbergen, J. Biomed. Opt. **12**, 024020 (2007).
5. D. J. Faber and T. G. van Leeuwen, Opt. Lett. **34**, 1435 (2009).
6. C. Xu, D. L. Marks, M. N. Do, and S. A. Boppart, Opt. Express **12**, 4790 (2004).
7. B. Hermann, K. Bizheva, A. Unterhuber, B. Povazay, H. Sattman, L. Schmetterer, A. F. Fercher, and W. Drexler, Opt. Express **12**, 1677 (2004).
8. A. Dubois, J. Moreau and C. Boccara, Opt. Express **16**, 17082 (2008).
9. D. T. Delpy, M. Cope, P. van der Zee, S. Arridge, S. Wray, and J. Wyatt, Phys. Med. Biol. **33**, 1433 (1988).
10. T. H. Pham, O. Coquoz, J. B. Fishkin, E. Anderson, and B. J. Tromberg, Rev. Sci. Instrum. **71**, 2500 (2000).
11. A. J. Welch and M. J. C. van Gemert, *Optical-Thermal Response of Laser-Irradiated Tissue* (Plenum, 1995).
12. D. A. Boas, K. K. Bizheva, and A. M. Siegel, Opt. Lett. **23**, 319 (1998).
13. A. L. Petoukhova, W. Steenbergen, T. G. van Leeuwen, and F. F. M. de Mul, Appl. Phys. Lett. **81**, 595 (2002).